International Journal of Science and Research (IJSR)
ISSN (Online): 2319-7064
Index Copernicus Value (2013): 6.14 | Impact Factor (2013): 4.438

Identification and Location of Faults in Three Phase Underground Power Cables by using Mexican Hat and Coif Let Wavelet Transform

D. Prabhavathi[1], K. Prakasam[2], Dr. M. Suryakalavathi[3], Dr. B. Ravindranath Reddy[4]

[1,]Sri Sivani Institute of Technology Srikakulam, Andhra Pradesh, India

[2,]Sri Sivani College of Engineering Srikakulam, Andhra Pradesh, India

[3,]Jawaharlal Nehru Technological University, Kukatpally, Hyderabad, Andhra Pradesh, India

[4]Jawaharlal Nehru Technological University, Kukatpally, Hyderabad, Andhra Pradesh, India

Abstract: ***Estimation and d termination of fault in an underground cable is very important in order to clear the fault quickly and to restore the supply with minimum interruption. This paper presents determination and location of fault in underground cables by wavelet transform as it is one of the most efficient tools for analyzing non stationary signals and it has been widely used in electrical power systems .The cable is modeled in MAT LAB simulink using simpower system tool box. Mexican hat and coif let wavelet transforms are used to extract the signals and the waveform are shown .The simulation results show that this method is efficient and powerful tool to estimate the faults when they occurs in the underground cables.***

Keywords: Underground cable, Fault Location, Wavelet Transform, power system disturbances, Mexican hat, and coif let

1. Introduction

In the modern electrical power systems of transmission and distribution systems, underground cable is used largely in urban areas and compared to overhead lines, fewer faults occur in underground cables. However if faults occur, it's difficult to repair and locate the fault. Faults that could occur on underground cables networks are single phase-to-earth (LG) fault; double phase-to-earth (LLG) fault and three phase-to-earths (LLLG) fault [1]. The single line to earth fault is the most common fault type and occurs most frequently. Fault detection and location based on the fault induced current or voltage travelling waves has been studied for years together. In all these techniques, the location of the fault is determined using the high frequency transients [1]. . Fault location based on the travelling waves can generally be categorized into two: single-ended and double ended. For single-ended, the current or voltage signals are measured at one end of the line and fault location relies on the analysis of these signals to detect the reflections that occur between the measuring point and the fault. For the double-ended method, the time of arrival of the first fault generated signals are measured at both ends of the lines using synchronized timers [2]

2. Wavelet Transform

The wavelet transform is similar to the Fourier transform (or much more to the windowed Fourier transform) with a completely different merit function. The main difference is this: Fourier transform decomposes the signal into sines and cosines, i.e. the functions localized in Fourier space; in contrary the wavelet transform uses functions that are localized in both the real and Fourier space. Generally, the wavelet transform can be expressed by the following equation:

$$F(a,b) = \int_{-\infty}^{\infty} f(x)\varphi * (a,b)(x)dx \qquad (1)$$

where the * is the complex conjugate symbol and function ψ is some function. This function can be chosen arbitrarily provided that obeys certain rules. As it is seen, the Wavelet transform is in fact an infinite set of various transforms, depending on the merit function used for its computation. This is the main reason, why we can hear the term "wavelet transforms" in very different situations and applications. There are also many ways how to sort the types of the wavelet transforms. Here we show only the division based on the wavelet orthogonality. We can use *orthogonal wavelets* for discrete wavelet transform development and *non-orthogonal wavelets* for continuous wavelet transform development. These two transforms have the following properties:

The discrete wavelet transform returns a data vector of the same length as the input is. Usually, even in this vector many data are almost zero. This corresponds to the fact that it decomposes into a set of wavelets (functions) that are orthogonal to its translations and scaling. Therefore we decompose such a signal to a same or lower number of the wavelet coefficient spectrum as is the number of signal data points. Such a wavelet spectrum is very good for signal processing and compression, for example, as we get no redundant information here. The continuous wavelet transforms in contrary returns an array one dimension larger than the input data. For a 1D data we obtain an image of the time-frequency plane. We can easily see the signal frequencies evolution during the duration of the signal and compare the spectrum with other signals spectra. As here is used the non-orthogonal set of wavelets, data are correlated highly, so big redundancy is seen here. This helps to see the results in a more humane form.

2.1 Discrete Wavelet Transform

The discrete wavelet transform (DWT) is an implementation of the wavelet transform using a discrete set of the wavelet scales and translations obeying some defined rules. In other words, this transform decomposes the signal into mutually orthogonal set of wavelets, which is the main difference from the continuous wavelet transform (CWT), or its implementation for the discrete time series sometimes called discrete-time continuous wavelet transform (DT-CWT). The wavelet can be constructed from a scaling function which describes its scaling properties. The restriction that the scaling functions must be orthogonal to its discrete translations implies some mathematical conditions on them which are mentioned everywhere, e.g. the dilation equation

$$\varphi(x) = \sum_{k=-\infty}^{\infty} ak\varphi(Sx - K) \quad (2)$$

Where S is a scaling factor (usually chosen as 2). Moreover, the area between the function must be normalized and scaling function must be orthogonal to its integer translations, i.e.

$$\int_{-\infty}^{\infty} \emptyset(x)\emptyset(x+l)dx = \delta 0,l \quad (3)$$

After introducing some more conditions (as the restrictions above does not produce unique solution) we can obtain results of all these equations, i.e. the finite set of coefficients a_k that define the scaling function and also the wavelet. The wavelet is obtained from the scaling function as N where N is an even integer. The set of wavelets then forms an orthonormal basis which we use to decompose the signal. Note that usually only few of the coefficients a_k are nonzero, which simplifies the calculations.

2.2 Continuous Wavelet Transform

Like the Fourier transform, the continuous wavelet transform (CWT) uses inner products to measure the similarity between a signal and an analyzing function. In the Fourier transform, the analyzing functions are complex exponentials; $e^{j\omega t}$ The resulting transform is a function of a single variable, ω. In the short-time Fourier transform, the analyzing functions are windowed complex exponentials, W (t) $e^{j\omega t}$ and the result in a function of two variables.The STFT coefficients, F(ω,τ) represent the match between the signal and a sinusoid with angular frequency ω in an interval of a specified length centered at τ.In the CWT, the analyzing function is a wavelet, ψ. The CWT compares the signal to shifted and compressed or stretched versions of a wavelet. Stretching or compressing a function is collectively referred to as dilation or scaling and corresponds to the physical notion of *scale*. By comparing the signal to the wavelet at various scales and positions, you obtain a function of two variables. The two-dimensional representation of a one-dimensional signal is redundant. If the wavelet is complex-valued, the CWT is a complex-valued function of scale and position. If the signal is real-valued, the CWT is a real-valued function of scale and position. For a scale parameter, a>0, and position, *b*, the CWT is:

$$c(a,b;f(t),\psi(t)) = \int_{-\infty}^{\infty} f(t)\frac{1}{\sqrt{a}}\,\psi*\frac{(t-b)}{a}dt \quad (4)$$

where * denotes the complex conjugate. Not only do the values of scale and position affect the CWT coefficients, the choice of wavelet also affects the values of the coefficients. By continuously varying the values of the scale parameter, *a*, and the position parameter, *b*, you obtain the *CWT Coefficients C(a,b)*. Note that for convenience, the dependence of the CWT coefficients on the function and analyzing wavelet has been suppressed. Multiplying each coefficient by the appropriately scaled and shifted wavelet yields the constitute wavelets of the original signal.

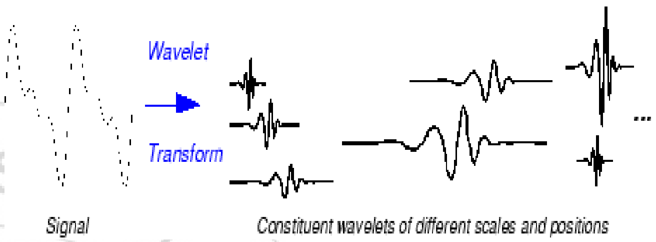

There are many different admissible wavelets that can be used in the CWT. While it may seem confusing that there are so many choices for the analyzing wavelet, it is actually a strength of wavelet analysis. Depending on what signal features you are trying to detect, you are free to select a wavelet that facilitates your detection of that feature. For example, if you are trying to detect abrupt discontinuities in your signal, you may choose one wavelet. On the other hand, if you are interesting in finding oscillations with smooth onsets and offsets, you are free to choose a wavelet that more closely matches that behavior.

3. Identification and Location of Faults

By comparing the transient signals at all phases the classification of fault can be made .If the transient signal appears at only one phase then the fault is single line to ground fault The transient signals generated by the fault is no stationary and is of wide band of frequency, when fault occurs in the network, the generated transient signals travels in the network. On the arrival at a discontinuity position, the transient wave will be partly reflected and the remainder is incident to the line impedance. The transient reflected from the end of the line travels back to the fault point where another reflection and incident occur due to the discontinuity of impedance. To capture these transient signals wavelet analysis can be used. The fault location can be carried out by comparing the aerial mode wavelet coefficient to determine the time instant when the energy of the signal reaches its peak value. The distance between the fault point and the bus of the faulted branch is calculated as follows consider a three phase cable line of length X connected between bus A and bus B, with a characteristic impedance Zc and traveling wave velocity of v. If a fault occurs at a distance X_2 from bus A, this will appear as an abrupt injection at the fault point. This injection will travel like a wave "surge" along the line in both directions and will continue to bounce back and forth between fault point, and the two terminal buses until the post-fault steady state is reached. The distance to the fault point can be calculated bu using travelling wave theory. Let t_1 and t_2 corresponds to the times at which the modal signals wavelet coefficients in scale 1, show their initial peaks for signals recorder at bus A and bus B. the delay between the fault detection times at the two ends is $t_l - t_2$ be determined. When td is determined we could obtain the fault location from bus A According to:

$$X_2 = X- (t_1-t_2)\ V/2 \qquad (5)$$

Or from bus B

$$X_1 = X - (t_2- t_1)\ V/2 \qquad (6)$$

The v is assumed to be 1.8182x105 miles/sec, Sampling time is 10 us and the total line length is 100km. Where X_1 and X_2 is the distance to the fault, td is the time difference between two consecutive peaks of the wavelet transform coefficients of the recorded current and v is the wave propagation velocity.

3.1 Method of Simulation

First 220 KV, 100km underground cable is modeled in MAT LAB Simulink with 7.8 versions and response of the complete system is evaluated for different faults. Wavelet transform effectively acts as a band pass filter which extracts a band of high frequency transient current signals from the faulted cable. The total length of the cable considered is 100km. Results from simulations are obtained with 800 Hz sampling rate and with Wavelet transform of Mexican hat and Coif let. The travelling wave velocity of the signals in the 220 kV underground cable system is 1.8182×10^5 km/s, and sampling time of 10µs is used. Fig 1 depicts the single line diagram of the simulated system which is 220KV, 50Hz, 100 km underground power cable.

3 Phase source 3 Phase load

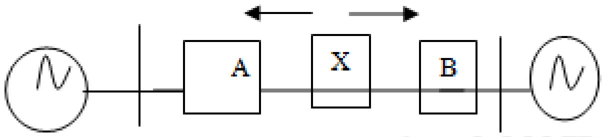

Figure 1: Three - Phase underground cable Transmission line

4. Scheme of Evaluation

In this paper the authors select all the possible cases to illustrate the performance of the proposed technique under fault conditions. First LG fault is selected as simulation case and fault locations are tabulated along with % error to compare the deviation from the actual values using continuous wavelet transform (both MEXICAN HAT AND COIF LET). Similarly for simulation and their results are tabulated. LLG and LLLG faults selected. The results of error between the Mexican hat and Coif let wavelet transforms are tabulated in table 1, Table 2 and table 3. Since the impedance of the total line length is a known quantity, the distance to the fault will be obtained proportional to the imaginary component of the measured impedance. The overall flowchart of the proposed algorithm is shown in

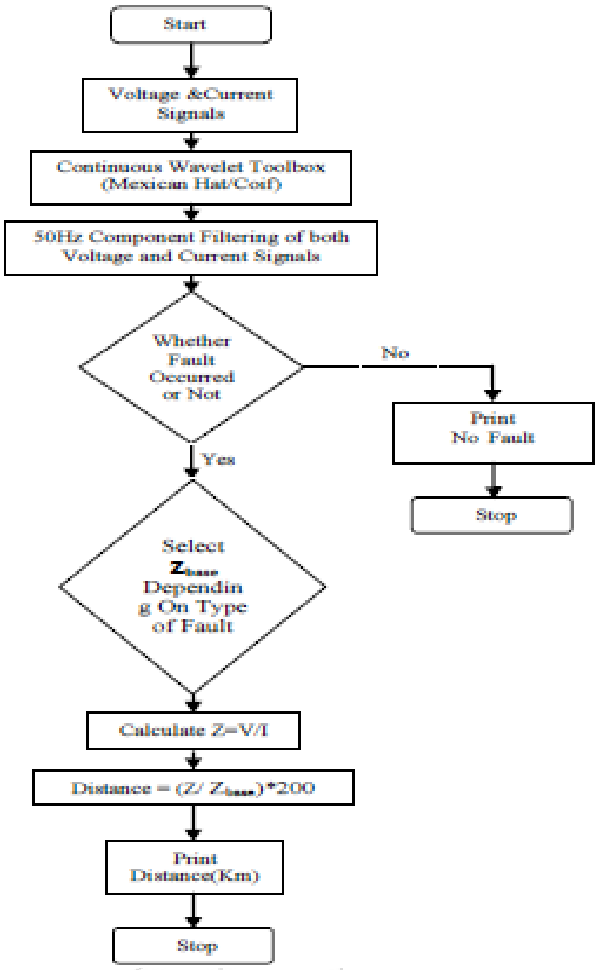

Figure 2: The overall flowchart of the proposed algorithm

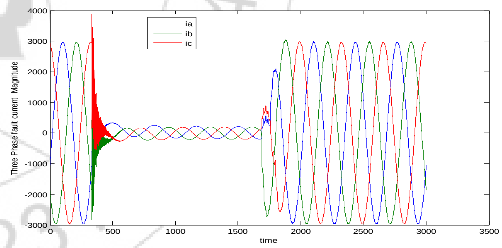

Figure 3: Three Phase current for LLLG fault at 25 km

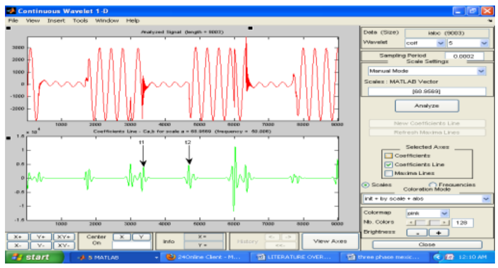

Figure 4: Three Phase current for LLLG fault at 25 km (Coif Let)

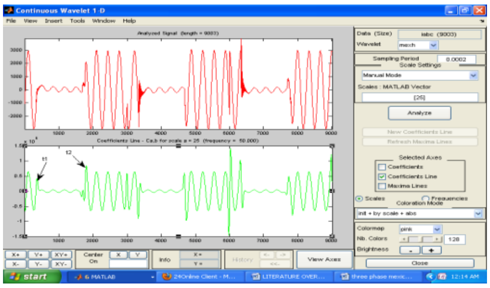

Figure 5: Three Phase current for LLLG fault at 25 km (Mexican Hat)

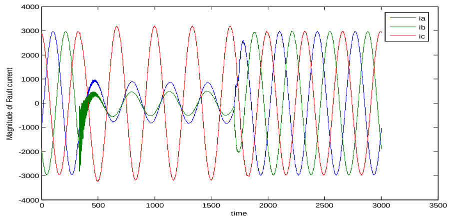

Figure 6: Two Phase current for LLG fault at 25 km

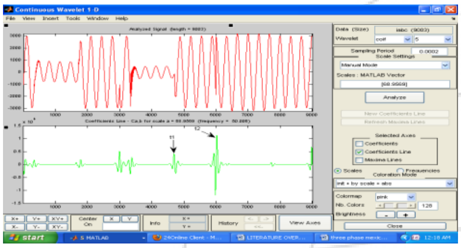

Figure 7: Two Phase current for LLG fault at 25 km (Coif Let)

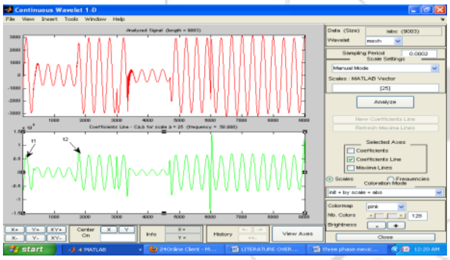

Figure 8: Two Phase current for LLG fault at 25 km (Mexican Hat)

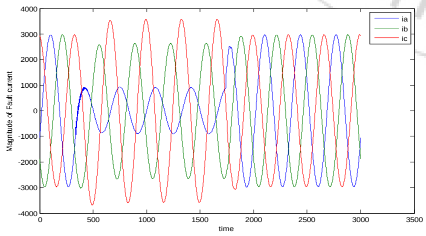

Figure 9: TSingle Phase current for LG fault at 25 km

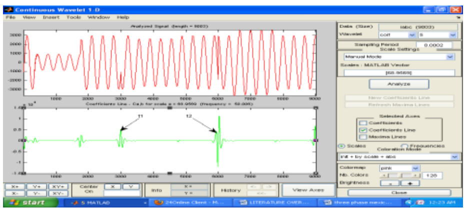

Figure 10: Single Phase current for LG fault at 25 km (Coif Let)

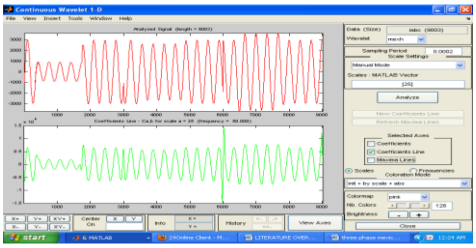

Figure 11: Single Phase current for LLG fault at 25 km (Mexican Hat)

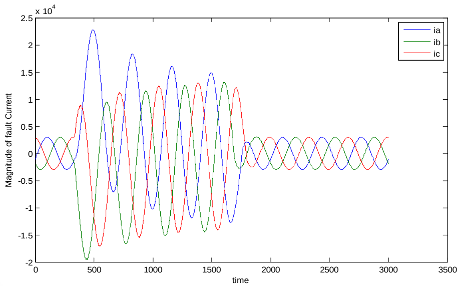

Figure 12: TThree Phase current for LLG fault at 50 km

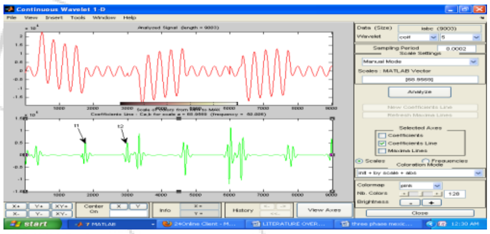

Figure 13: TThree Phase current for LLLG fault at 50 km (Coif Let)

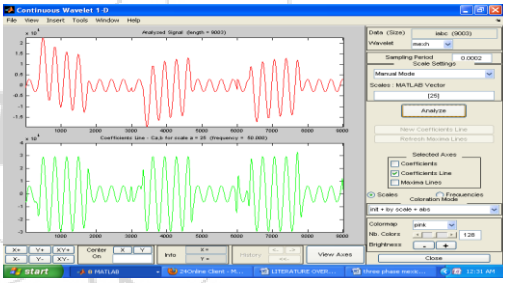

Figure 14: Three Phase current for LLLG fault at 50 km (Mexican Hat)

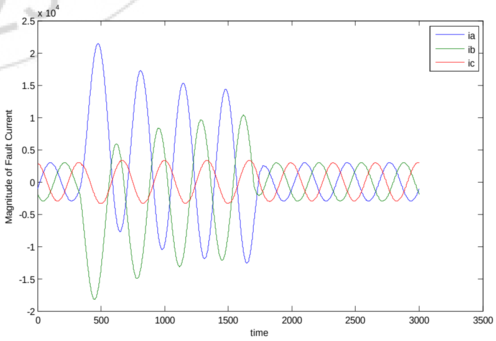

Figure 15: Two Phase current for LLG fault at 50 km

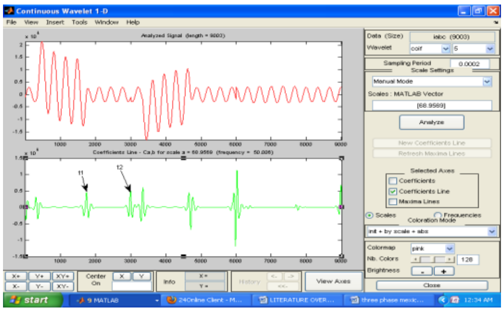

Figure 16: Two Phase current for LLG fault at 50 km (Coif Let)

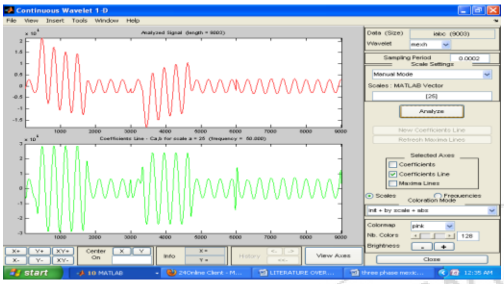

Figure 17: Two Phase current for LLG fault at 50 km (Mexican Hat)

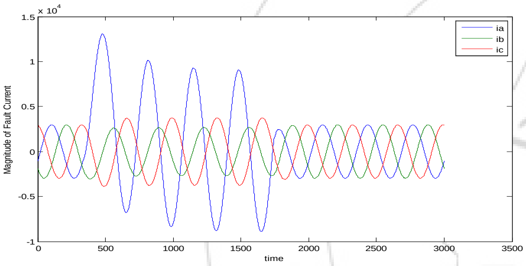

Figure 18: Single Phase current for LG fault at 50 km

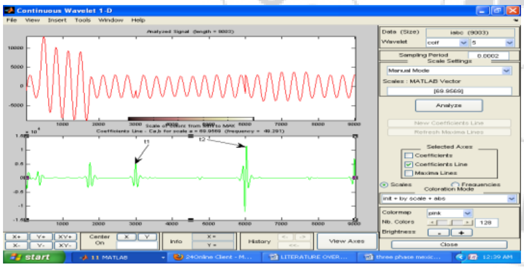

Figure 19: Single Phase current for LG fault at 50 km (Coif Let)

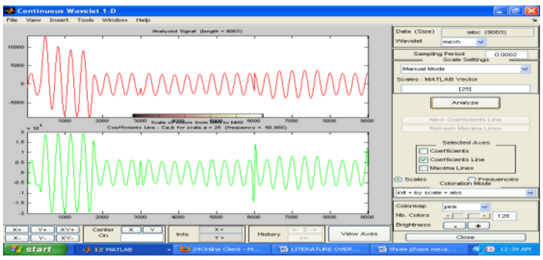

Figure 20: Single Phase current for LG fault at 50 km (Mexican Hat)

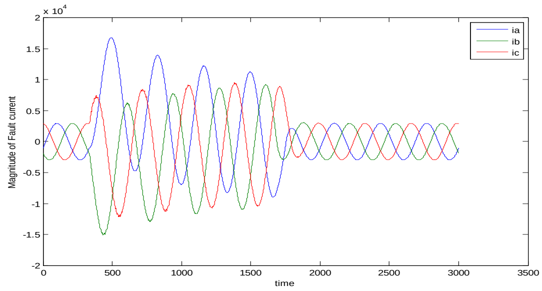

Figure 21: TThree Phase current for LLLG fault at 75 km

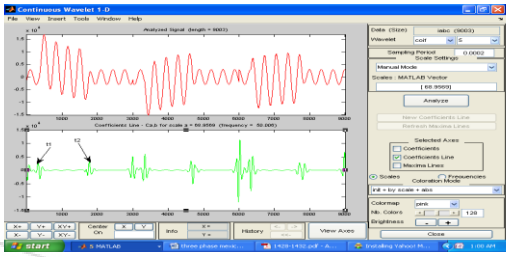

Figure 22: TThree Phase current for LLLG fault at 75 km(Coif Let)

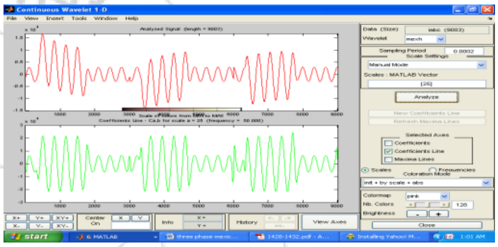

Figure 23: TThree Phase current for LLLG fault at 75 km(Coif Let)

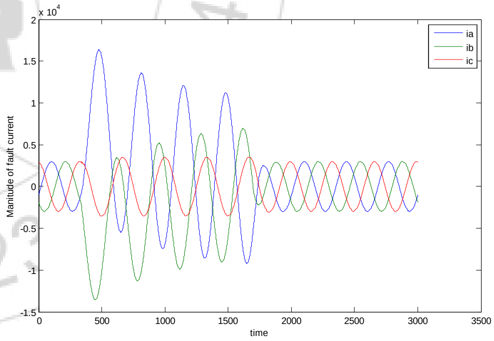

Figure 24: Two Phase current for LLG fault at 75 km

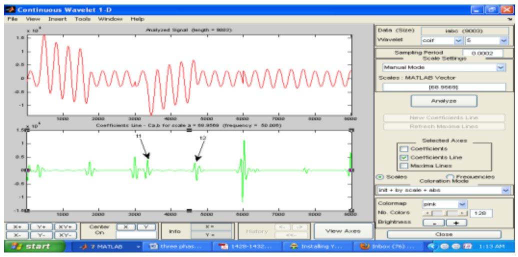

Figure 25: Two Phase current for LLG fault at 75 km(Coif Let)

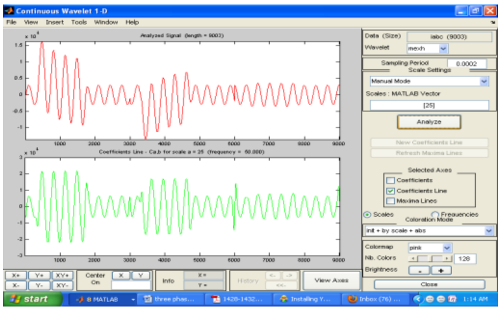

Figure 26: TTwo Phase current for LLG fault at 75 km(Mexican Hat)

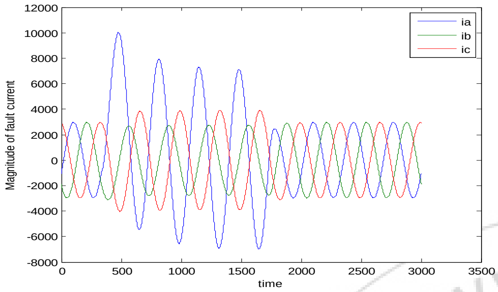

Figure 27: Single phase Phase current for LG fault at 75 km(Coif Let)

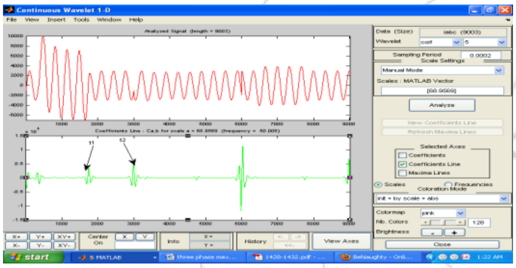

Figure 28: Single Phase Phase current for LG fault at 75 km(Coif Let)

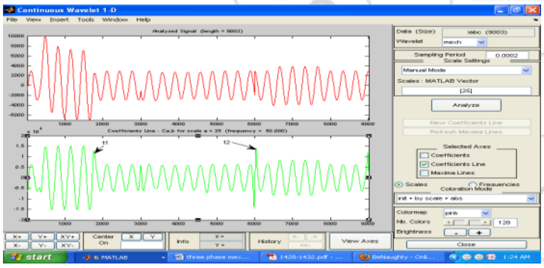

Figure 29: .Single Phase Phase current for LG fault at 75 km(Mexican Hat)

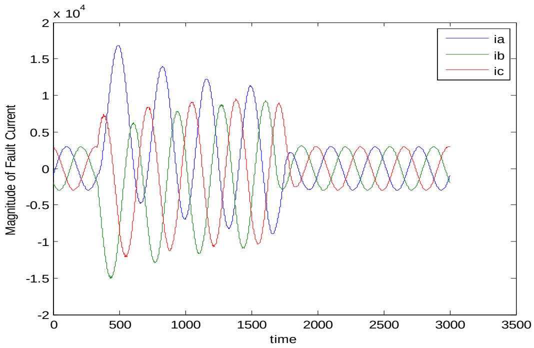

Figure 30: TThree Phase current for LLLG fault at 100 km

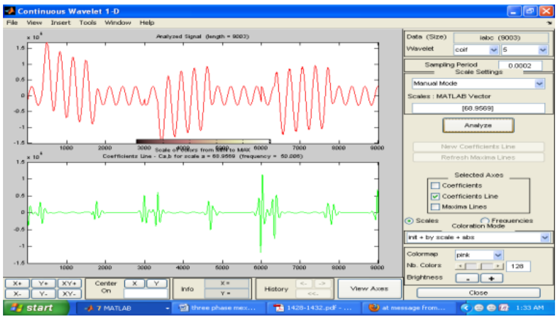

Figure 31: TThree Phase current for LLLG fault at 100 km(Coif Let)

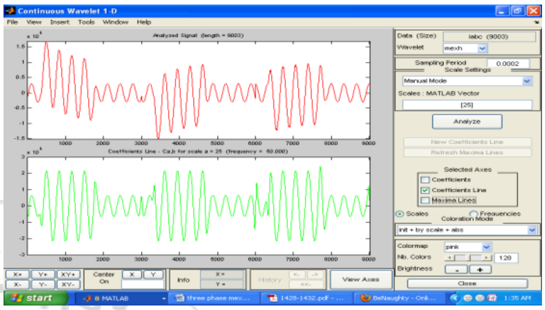

Figure 32: TThree Phase current for LLLG fault at 100 km(Mexican Hat)

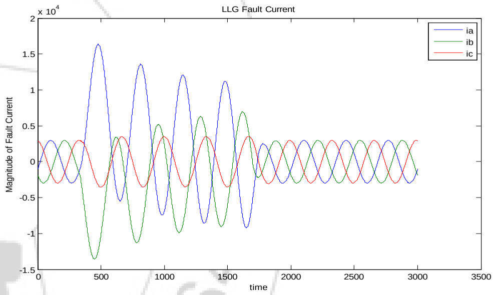

Figure 33: Two Phase current for LLG fault at 100 km

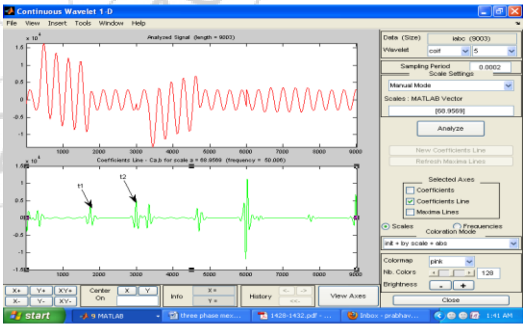

Figure 34: Two Phase current for LLG fault at 100 km(Coif Let)

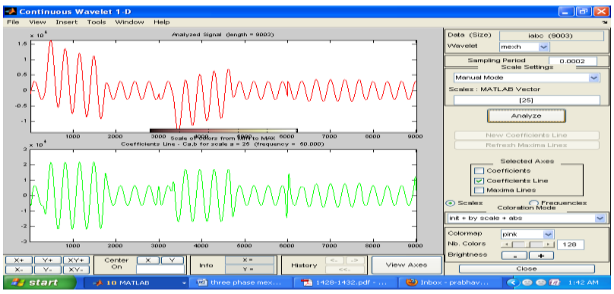

Figure 35: Two Phase current for LLG fault at 100 km(Mexican Hat)

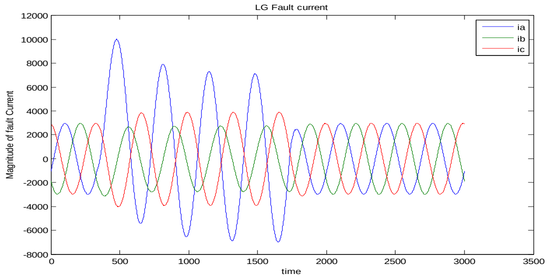

Figure 36: .Single Phase current for LG fault at 100 km

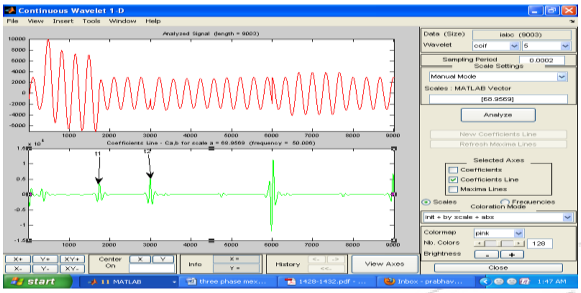

Figure 37: Single Phase current for LG fault at 100 km(Coif Let)

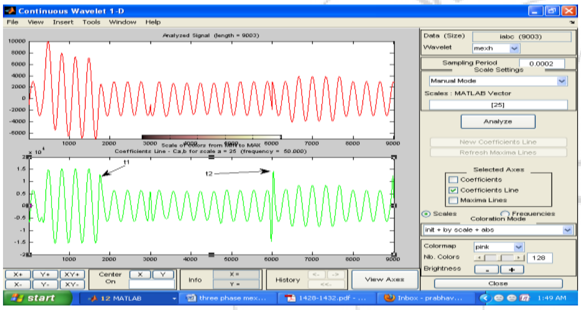

Figure 38: Single Phase current for LG fault at 100 km(Mexican Hat)

Table 1

LG Fault				
Actual Distance(km)	Distance (KM) Mexican Hat	Distance(KM) Coif Let	% Error Mexican Hat	% Error Coif Let
25	24.25	26.12	-3.0	4.48
50	52.23	51.84	3.6	3.68
75	75.26	74.69	-0.41	-0.413
100	104.87	107.64	4.87	9.74

Table 2

LLG Fault				
Actual Distance (km)	Distance(KM) Mexican Hat	Distance (KM) Coif Let	% Error Mexican Hat	% Error Coif Let
25	24.10	24.91	-3.6	-0.36
50	50.15	51.21	-0.36	2.42
75	73.56	74.52	-1.92	-0.64
100	103.62	105.73	-3.62	-5.73

Table 3

LLLG Fault				
Actual Distance (km)	Distance (KM) Mexican Hat	Distance (KM) Coif Let	% Error Mexican Hat	% Error Coif Let
25	23.15	24.54	-7.4	-1.84
50	52.31	53.1	6.42	6.2
75	75.96	76.21	1.2	1.613
100	101.52	106.85	1.52	6.85

5. Results and Conclusions

This paper presents a new Mexican hat and coif let wavelet transform based fault location. he transient signals generated by the fault is no stationary and is of wide band of frequency, when fault occurs in the network, the generated transient signals travels in the network. On the arrival at a discontinuity position, the transient wave will be partly reflected and the remainder is incident to the line impedance. The transient reflected from the end of the line travels back to the fault point where another reflection and incident occur due to the discontinuity of impedance. By traveling wave theory of Underground cable transmission lines, the transient signals are first decoupled into their modal components and then the signals transformed from the time domain into the time frequency domain by applying the wavelet transform both Mexican hat and Coif let. The wavelet transform coefficients at the two lowest scales then are used to determine the fault location using equations (5) and (6).The results obtained by both the wavelet transforms are tabulated along with the errors in the tables

Author Profile

D.Prabhavathi Born in 1976 August 27, her B.Tech degree from K.S.R.M College of Engineering, Kadapa, S.V University, and M.Tech degree from S.V university in the year 2003.She has specialized in Power Systems, High Voltage Engineering. Her research interests include Simulation studies on faults identification in UG cable of LT and HT. Fuzzy logic, High Voltage Engineering, Power Quality, FACTS Controllers; she has 14 years of experience. She has guided 21 M.Tech Projects and 54 Batch projects in various areas of engineering. She is presently working as Prof and H.O.D of Dept of E.E.E, Sri Sivani Institute of Technology , Srikakulam Andhrapradesh ,INDIA

K.Prakasam, Born in 1973 April 20, his B.tech degree from KSRM College of Engineering SV university in 1997 and M.Tech degree from SV university in the year 2004. He has specialised in Power Systems, High Voltage Engineering and Control Systems. His research interests include Simulation studies on Transients of different power system equipment. He has 16 years of experience. He is presently working as Prof and H.O.D of Dept of E.E.E, Sri Sivani College of Engineering ,Srikakulam, Andhra Pradesh, INDIA

Dr. M. Surya Kalavathi, Born on 8th July 1966, Obtained her B.Tech degree from S.V. U. in 1988 and M.Tech from S.V.U. in the year 1992. Obtained her doctoral degree from J.N.T.U, Hyderabad and Post Doctoral from CMU, USA. She is presently the Professor in the department of EEE, J.N.T.U.H College of Engineering J.N.T.U.H, Kukatpally, Hyderabad. Published 21 Research Papers and presently guiding many Ph.D. Scholars. She has specialized in Power Systems, High Voltage Engineering and Control Systems. Her research interests include Simulation studies on Transients of different power system equipment. She has 23 years of experience. She has invited for various lectures in repudiated institutes in and around Andhra Pradesh and Telangana colleges.

Bhumanapally Ravindhranath Reddy, Born on 3rd September, 1969. Got his B.Tech in Electrical & Electronics Engineering from the J.N.T.U. College of Engineering. Anantapur in the year 1991.Completed his M.Tech in Energy Systems in IPGSR of J.N.T.University Hyderabad in the year 1997. Obtained his doctoral degree from J.N.T.U.A,Anantapur University in the field of Electrical Power Systems. Published 12 Research Papers and presently guiding 6 Ph.D. Scholars. He was specialised in Power Systems, High Voltage Engineering and Control Systems. His research interests include Simulation studies on Transients of different power system equipment.

References

[1] A. Bonnaccorsi, "On the Relationship between Firm Size and Export Intensity," Journal of International Business Studies, XXIII (4), pp. 605-635, 1992. (journal style)
[2] R. Caves, Multinational Enterprise and Economic Analysis, Cambridge University Press, Cambridge, 1982. (book style)
[3] M. Clerc, "The Swarm and the Queen: Towards a Deterministic and Adaptive Particle Swarm Optimization," In Proceedings of the IEEE Congress on Evolutionary Computation (CEC), pp. 1951-1957, 1999. (conference style)
[4] H.H.Crokell,"Specialization and International Competitiveness," in Managing the Multinational Subsidiary, H. Etemad and L. S, Sulude (eds.), Croom-Helm, London, 1986. (book chapter style)
[5] K. Deb, S. Agrawal, A. Pratab, T. Meyarivan, "A Fast Elitist Non-dominated Sorting Genetic Algorithms for Multiobjective Optimization: NSGA II," KanGAL report 200001, Indian Institute of Technology, Kanpur,
[6] India, 2000. (technical report style)
[7] J. Geralds, "Sega Ends Production of Dreamcast," vnunet.com, para. 2, Jan. 31, 2001. [Online]. Available: http://nl1.vnunet.com/news/1116995. [Accessed: Sept. 12, 2004]. (General Internet site)